Opt Quant Electron (2012) 43:147–162
DOI 10.1007/s11082-011-9517-0

Symbolic computation on soliton solutions for variable-coefficient nonlinear Schrödinger equation in nonlinear optics

Wen-Jun Liu · Bo Tian

Received: 14 July 2011 / Accepted: 29 November 2011 / Published online: 23 December 2011

Abstract Soliton interaction and control using the dispersion-decreasing fibers with potential applications to the design of high-speed optical devices and ultralarge capacity transmission systems are investigated based on solving the variable-coefficient nonlinear Schrödinger equation with symbolic computation. Via the Hirota method, analytic two- and three-soliton solutions for that model are obtained, with their relevant properties and features illustrated. Dispersion-decreasing fibers with different profiles are found to be able to control the soliton velocity. Additionally, through the asymptotic analysis for the two-soliton solutions, we point out that the interaction between two solitons is elastic. Finally, a new approach to controll the soliton interaction using the dispersion-decreasing fiber with the Gaussian profile is suggested.

Keywords Soliton interaction · Soliton control · Variable-coefficient nonlinear Schrödinger equation · Symbolic computation

1 Introduction

It has been predicted theoretically (Hasegawa and Tappert 1973a,b) that an optical pulse in a dielectric fiber can form a soliton due to the balance between the nonlinearity and group velocity dispersion (GVD) effects. The theoretical results have been supported by the experimental demonstration of solitons (Mollenauer et al. 1980). Since then, the propagation of solitons has been the object of extensive studies (Agrawal 2007; Pusch et al. 2011; Gao and Tian 2007; Serkin et al. 2007; Ponomarenko and Agrawal 2007; Porsezian et al. 2009;

W.-J. Liu (✉) · B. Tian
State Key Laboratory of Information Photonics and Optical Communications, Beijing University of Posts and Telecommunications, Beijing 100876, China
e-mail: jungliu@bupt.edu.cn

W.-J. Liu · B. Tian
School of Science, Beijing University of Posts and Telecommunications, P. O. Box 122, Beijing 100876, China

Kanna et al. 2004), and the nonlinear Schrödinger (NLS)-typed equations have riveted the attention of researchers in long-distance optical fiber communications (Luo et al. 2009; Wu et al. 2008; Han and Park 2011). To enhance the communication quality of high-bit rate and long-distance optical communication systems, soliton interaction based on the NLS-typed equations have been worked out in nonlinear optics (Kodama and Nozaki 1987; Hasegawa and Matsumoto 2003; Ganapathy et al. 2008; Xie et al. 2002; Kivshar and Agrawal 2003; Kubota and Nakazawa 1993).

When solitons transmit in the optical fiber, it would be better if they could be well separated from each other (Hasegawa and Matsumoto 2003; Ganapathy et al. 2008). For this purpose, soliton width should be shorter than the bit rates. Hence, when compared with a linear pulse having the same bit rate, the soliton requires a larger bandwidth (Ganapathy et al. 2008) with the demand for the ultralarge capacity transmission systems (Morita et al. 1999). In order to achieve the high-bit rates in those systems, solitons are inputed close to each other, which leads to the mutual interaction of adjacent solitons (Pinto et al. 1998). The interaction between solitons may result in the reduction in the bandwidth of the soliton-based optical communication systems (Kodama and Nozaki 1987). Therefore, it is needed to investigate the mutual interaction between solitons as a step towards the realization of the ultralarge capacity transmission systems (Kurokawa et al. 1994).

The mutual interaction between solitons can lead to the distortion of a sequence of solitons, and therefore to induce the performance degradation of soliton transmission systems (Xie et al. 2002). The study of the physical effects leading to this deviation has been a subject of studies (Xie et al. 2002; Pinto et al. 1998; Morita et al. 1999; Kurokawa et al. 1994; Kubota and Nakazawa 1993; Komarova et al. 2007; Wabnitz et al. 1995; Georges and Favre 1993), such as the effect of soliton interaction on timing jitter in communication systems (Pinto et al. 1998). Additionally, it has been shown in Xie et al. (2002) that, for conventional soliton systems, although the single pulse has certain robustness to polarization-mode dispersion (PMD), interaction of solitons would seriously distort a sequence of pulses and make the soliton systems worse than the linear systems. Also, some controlling methods have already been worked out (Kubota and Nakazawa 1993; Komarova et al. 2007; Wabnitz et al. 1995; Georges and Favre 1993). For example, soliton transmission control, combining the synchronous modulation and a band pass filter, has been proposed for the realization of an ultralong distance soliton communication system (Kubota and Nakazawa 1993). A way to control the interaction of solitons in laser cavities has been suggested (Komarova et al. 2007). Other approaches, such as the phase and amplitude control of solitons, have also been introduced to overcome the interaction of solitons (Wabnitz et al. 1995; Georges and Favre 1993). Thus, the concept of soliton control in nonlinear dynamical systems described by the NLS-typed equations seems a necessary development in all optical soliton communications. Relevant issues can also be see in Sun et al. (2009, 2010); Wang et al. (2009, 2010); Yu et al. (2010, 2011).

The present paper will be devoted to the soliton interaction and control in the variable-coefficient NLS (vcNLS) equation with the effects of varying dispersion and nonlinearity. In order to realize the above effects, the dispersion-decreasing fiber (DDF) will be used, in which the magnitude of the GVD parameter decreases along the propagation direction of optical solitons (Wai and Cao 2003). In addition, the Hirota method (Hirota 1973) based on symbolic computation (Gao and Tian 2007) will make it possible to solve the vcNLS equation under the investigation. Moreover, via the soliton solutions obtained, aspects of soliton control will be discussed. Interaction scenarios pertaining to the different phase injection will be dealt with.

The structure of this paper will be as follows. In Sect. 2, with the aid of symbolic computation, the bilinear form for the vcNLS equation will be obtained. In Sect. 3, two- and three-soliton solutions will be presented based on the bilinear form, and the analysis of solitons will be illustrated. The conclusions of this paper will be given in Sect. 4.

2 Bilinear form for the vcNLS equation

Let us assume that the nonlinearity in the optical fiber is described by the Kerr effect. In a real communication system, the transmission of optical solitons could be described by the vcNLS equation (Serkin and Hasegawa 2000, 2002; Wang et al. 2005; Zhang et al. 2005; Li and Chen 2004; Chen et al. 2006),

$$i\,\frac{\partial E}{\partial \xi}+\frac{1}{2}\,D(\xi)\,\frac{\partial^2 E}{\partial \tau^2}+R(\xi)\,|E|^2\,E+i\,\Gamma(\xi)\,E=0, \tag{1}$$

where $E(\xi,\tau)$ is the complex envelope of the electrical field in the moving frame with ξ as the normalized distance of propagation along the fiber and τ as the retarded time, $D(\xi)$ represents the GVD coefficient, $R(\xi)$ is the nonlinearity parameter, and $\Gamma(\xi)$ is the amplification or absorption coefficient. Using the transformation (Tian and Gao 2005)

$$E(\xi,\tau)=\exp\left[-\int\Gamma(\xi)\,d\xi\right]u(\xi,\tau), \tag{2}$$

Eq. (1) can be simplified as (Turitsyn et al. 1998; Inoue et al. 2000; Lakoba and Agrawal 2000)

$$i\,\frac{\partial u}{\partial \xi}+\frac{1}{2}\,p(\xi)\,\frac{\partial^2 u}{\partial \tau^2}+\sigma(\xi)\,|u|^2\,u=0, \tag{3}$$

with

$$p(\xi)=D(\xi),\quad \sigma(\xi)=R(\xi)\exp\left\{-\int\left[\Gamma(\xi)+\Gamma^*(\xi)\right]d\xi\right\}. \tag{4}$$

Hereby, the asterisk denotes the complex conjugate.

With the dependent variable transformation (Hirota 1973):

$$u=\frac{g(\xi,\tau)}{f(\xi,\tau)}, \tag{5}$$

where $g(\xi,\tau)$ is a complex differentiable function and $f(\xi,\tau)$ is a real one, after some symbolic manipulations, the bilinear form for Eq. (3) is obtained as

$$\left[i\,D_\xi+\frac{1}{2}\,p(\xi)\,D_\tau^2\right]g\cdot f=0\,, \tag{6}$$

$$D_\tau^2 f\cdot f=2\,|g|^2, \tag{7}$$

with the coefficient constraint (Serkin and Hasegawa 2000, 2002; Wang et al. 2005; Zhang et al. 2005; Li and Chen 2004; Chen et al. 2006)

$$\sigma(\xi)=p(\xi), \tag{8}$$

which is a special case for Eq. (3) to be Painlevé-integrable (Joshi 1987). Hereby, Hirota's bilinear operators D_ξ and D_τ (Hirota 1971) are defined by

$$D_\xi^m D_\tau^n (a \cdot b) = \left(\frac{\partial}{\partial \xi} - \frac{\partial}{\partial \xi'} \right)^m \left(\frac{\partial}{\partial \tau} - \frac{\partial}{\partial \tau'} \right)^n a(\xi, \tau)\, b(\xi', \tau') \Big|_{\xi'=\xi, \tau'=\tau}. \tag{9}$$

Equations (6) and (7) can be solved with the following power series expansions for $g(\xi, \tau)$ and $f(\xi, \tau)$:

$$g(\xi, \tau) = \varepsilon\, g_1(\xi, \tau) + \varepsilon^3\, g_3(\xi, \tau) + \varepsilon^5\, g_5(\xi, \tau) + \cdots, \tag{10}$$
$$f(\xi, \tau) = 1 + \varepsilon^2\, f_2(\xi, \tau) + \varepsilon^4\, f_4(\xi, \tau) + \varepsilon^6\, f_6(\xi, \tau) + \cdots, \tag{11}$$

where ε is a formal expansion parameter. Substituting Eqs. (10) and (11) into Eqs. (6) and (7) and equating coefficients of the same powers of ε to zero yields the recursion relations for $f_n(\xi, \tau)$'s and $g_n(\xi, \tau)$'s $(n = 1, 2, \ldots)$.

3 Soliton solutions and discussions

In the above section, we have obtained the bilinear form for Eq. (3). In order to analytically study the propagation of solitons, now we present the soliton solutions from Eqs. (6) and (7). For understanding how the variable coefficients affect the velocity of solitons, we will graphically analyze some special cases.

3.1 Two-soliton solutions

To obtain the two-soliton solutions for Eq. (3), we assume that

$$g_1(\xi, \tau) = e^{\theta_1} + e^{\theta_2}, \tag{12}$$

where $\theta_j = \eta_j\, \tau + k_j(\xi) + \varphi_j\ (j = 1, 2)$, $\eta_j = \eta_{jR} + i\, \eta_{jI}$, $k_j(\xi) = k_{jR}(\xi) + i\, k_{jI}(\xi)$, R and I represent the real and imaginary parts, respectively, η_{jR}, η_{jI}, φ_j are all real constants, and $k_{jR}(\xi)$, $k_{jI}(\xi)$ are differentiable functions to be determined. Substituting $g_1(\xi, \tau)$ into the resulting set of linear partial differential equations, and after some calculations, the constraints on the parameters of $k_{jR}(\xi)$ and $k_{jI}(\xi)$ appear to be

$$k_{jR}(\xi) = -\eta_{jR}\, \eta_{1I} \int p(\xi)\, d\xi, \quad k_{jI}(\xi) = \frac{\eta_{jR}^2 - \eta_{jI}^2}{2} \int p(\xi)\, d\xi,$$

and

$$\begin{aligned}
&g_3(\xi, \tau) = A_{21} e^{\theta_1 + \theta_2 + \theta_1^*} + A_{22} e^{\theta_1 + \theta_2 + \theta_2^*}, \\
&f_2(\xi, \tau) = B_{21} e^{\theta_1 + \theta_1^*} + B_{22} e^{\theta_2 + \theta_1^*} + B_{23} e^{\theta_1 + \theta_2^*} + B_{24} e^{\theta_2 + \theta_2^*}, \\
&f_4(\xi, \tau) = C_{21} e^{\theta_1 + \theta_2 + \theta_1^* + \theta_2^*}, \\
&g_n(\xi, \tau) = 0 \ \ (n = 5, 7, \ldots), \\
&f_n(\xi, \tau) = 0 \ \ (n = 6, 8, \ldots)
\end{aligned}$$

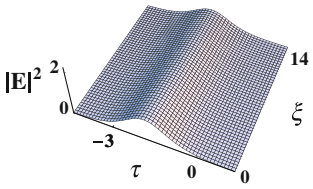

Fig. 1 Intensity profile of the soliton via Solutions (13). The parameters are $\Gamma(\xi) = 0.01$, $\eta_{1R} = \eta_{2R} = 1$, $\eta_{1I} = \eta_{2I} = 0$ and $\varphi_1 = \varphi_2 = 1.8$

with

$$A_{21} = \frac{(\eta_2 - \eta_1)^2}{(\eta_1 + \eta_1^*)^2(\eta_2 + \eta_1^*)^2}, \quad A_{22} = \frac{(\eta_1 - \eta_2)^2}{(\eta_2 + \eta_2^*)^2(\eta_1 + \eta_2^*)^2},$$
$$B_{21} = \frac{1}{(\eta_1 + \eta_1^*)^2}, \quad B_{22} = \frac{1}{(\eta_2 + \eta_1^*)^2}, \quad B_{23} = \frac{1}{(\eta_1 + \eta_2^*)^2}, \quad B_{24} = \frac{1}{(\eta_2 + \eta_2^*)^2},$$
$$C_{21} = \frac{(\eta_1 - \eta_2)^2\,(\eta_1^* - \eta_2^*)^2}{(\eta_1 + \eta_1^*)^2\,(\eta_2 + \eta_2^*)^2\,(\eta_1 + \eta_2^*)^2\,(\eta_2 + \eta_1^*)^2},$$

where the asterisk denotes the complex conjugate. Without loss of generality, we set $\varepsilon = 1$ and the two-soliton solutions can be explicitly expressed as

$$u = \frac{g(\xi,\tau)}{f(\xi,\tau)} = \frac{g_1(\xi,\tau) + g_3(\xi,\tau)}{1 + f_2(\xi,\tau) + f_4(\xi,\tau)}$$
$$= \frac{e^{\theta_1} + e^{\theta_2} + A_{21}e^{\theta_1+\theta_2+\theta_1^*} + A_{22}e^{\theta_1+\theta_2+\theta_2^*}}{1 + B_{21}e^{\theta_1+\theta_1^*} + B_{22}e^{\theta_2+\theta_1^*} + B_{23}e^{\theta_1+\theta_2^*} + B_{24}e^{\theta_2+\theta_2^*} + C_{21}e^{\theta_1+\theta_2+\theta_1^*+\theta_2^*}}. \quad (13)$$

Based on Solutions (13), we will graphically analyze how the features of solitons are affected by the choices of different dispersion profiles of the DDF and parameters.

3.1.1 The effect of η_{jR}

In order to investigate the effect of η_{jR}, we assume that $\eta_{jI} = 0$. The corresponding phenomena can be seen in Fig. 1.

Because $\eta_{1R} = \eta_{2R}$, the two solitons are combined into one soliton in Fig. 1, and the soliton interaction is eliminated. At this time, the effect of self-phase modulation (SPM) can cancel the effect of GVD perfectly. Because there exist fiber losses, the amplitude of the solitons has attenuated during the propagation. In fact, when $\eta_1 = \eta_2$, Solutions (13) can be simplified as

$$E = 2\,|\eta_{1R}|\,e^{i\,\eta_{1I}\tau + \frac{1}{2}\,i\,(\eta_{1R}^2 - \eta_{1I}^2)\int p(\xi)\,d\xi - \int \Gamma(\xi)\,d\xi}$$
$$\times \operatorname{sech}\left[\eta_{1R}\,\tau - \eta_{1R}\,\eta_{1I}\int p(\xi)\,d\xi + \varphi_0 - \ln(2\,|\eta_{1R}|)\right]. \quad (14)$$

Thus, the soliton amplitude is determined by η_{jR} and $\Gamma(\xi)$. Attention should be paid that $p(\xi)$ is not assigned a value in Fig. 1, because the effect of $p(\xi)$ disappears when η_{1I} is chosen to be zero in Expression (14), by contrast, $\eta_{1R} \neq \eta_{2R}$, interaction between two solitons can be seen in Figs. 2, 3, 4, 5.

Figures 2, 3, 4, 5 display the soliton propagation in different types of optical fibers. In Fig. 2, $p(\xi)$ is chosen as a constant, which indicates that the effect of GVD keeps constant during the propagation. Solitons follow a periodic evolution pattern as they propagate along the optical fibers in the anomalous dispersion regime. They first contract to a fraction of their

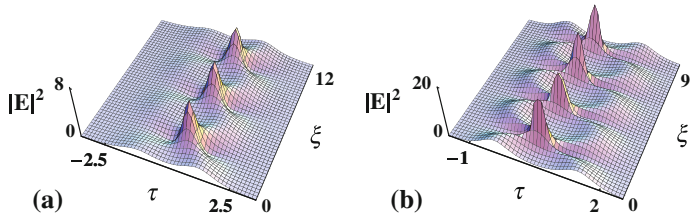

Fig. 2 Intensity profiles of solitons expressed via Solutions (13). The parameters are $\Gamma(\xi) = 0.01$, $\eta_{1I} = \eta_{2I} = 0$, $\varphi_1 = \varphi_2 = 1.8$, $p(\xi) = 1$, **a** $\eta_{1R} = 1$ and $\eta_{2R} = 2$, **b** $\eta_{1R} = 3$ and $\eta_{2R} = 2$

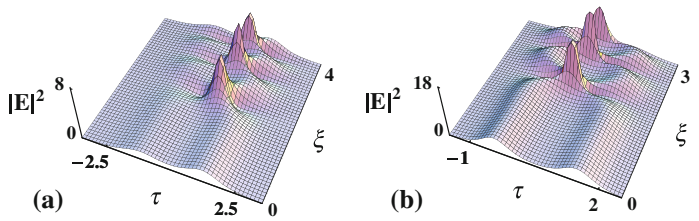

Fig. 3 Evolution of solitons via Solutions (13) with the linear profile of the DDF. The parameters are $\Gamma(\xi) = 0.01$, $\eta_{1I} = \eta_{2I} = 0$, $\varphi_1 = \varphi_2 = 1.8$, $p(\xi) = \left|1 + (\frac{1}{18} - 1)\xi\right|$, **a** $\eta_{1R} = 1$ and $\eta_{2R} = 2$, **b** $\eta_{1R} = 3$ and $\eta_{2R} = 2$

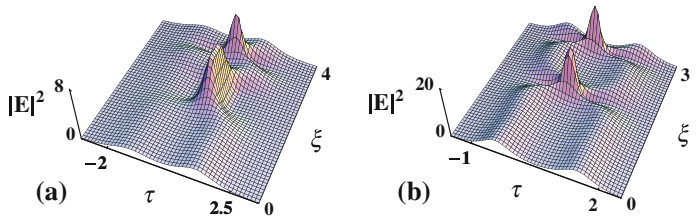

Fig. 4 Evolution of solitons via Solutions (13) with the cosine profile of the DDF. The parameters are $\Gamma(\xi) = 0.01$, $\eta_{1I} = \eta_{2I} = 0$, $\varphi_1 = \varphi_2 = 1.8$, $p(\xi) = \left|\cos\left[(\arccos\frac{1}{18})\,\xi\right]\right|$, **a** $\eta_{1R} = 1$ and $\eta_{2R} = 2$, **b** $\eta_{1R} = 3$ and $\eta_{2R} = 2$

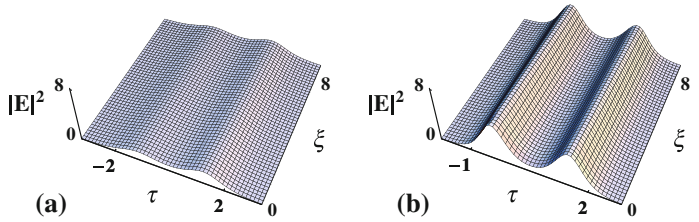

Fig. 5 Evolution of solitons via Solutions (13) with the Gaussian profile of the DDF. The parameters are $\Gamma(\xi) = 0.01$, $\eta_{1I} = \eta_{2I} = 0$, $\varphi_1 = \varphi_2 = 1.8$, $p(\xi) = \left|\exp\left[-(\ln 18)\,\xi^2\right]\right|$, **a** $\eta_{1R} = 1$ and $\eta_{2R} = 2$, **b** $\eta_{1R} = 3$ and $\eta_{2R} = 2$

initial width, and then merge again to recover the original shapes. Those changes result from the mutual interaction between the SPM and GVD (Wu et al. 2008). The SPM generates a frequency chirp such that the leading edge of the soliton is red-shifted while its trailing-edge

is blue-shifted from the central frequency and induces spectral broadening. However, the anomalous GVD contracts the solitons as they are positively chirped. As a result, the intensity near their central part is substantially increased. Because of the increasing intensity of solitons, the effect of SPM becomes stronger, which makes the solitons recover their original state after the interaction. The variation period and interaction time of solitons in Fig. 2b are shorter than those in Fig. 2a due to the increase of η_{1R} which intensifies the mutual interaction.

Different from Fig. 2, the steady transmission for two solitons in Figs. 3, 4 can be achieved in a short distance at first, and then the soliton interaction occurs periodically. The various change patterns of solitons can be explained by different choices of $p(\xi)$. The function $p(\xi)$ has been chosen according to the dispersion profile of the DDF in which the magnitude of the GVD parameter $|\beta_2(\xi)|$ decreases along the propagation direction. In Figs. 3a, 4a, the dispersion profiles of the DDF are the linear and cosine ones, respectively. Because $|\beta_2(\xi)|$ has little change at the beginning of the propagation, the effect of GVD is compensated by the SPM effect. When solitons propagate a certain distance, the effect of SPM plays a dominant role in the propagation, as a result, solitons interact with each other and appear the periodical changes. In Figs. 3b, 4b, the conclusion we derived from Fig. 2b is further strengthened. A fascinating phenomenon is shown in Fig. 5 that solitons do not interact with each other and transmit stably even if there exists an overlapping part between them. And this is exactly what we want in the ultralarge capacity transmission systems.

Therefore, the bigger the value of η_{jR} is, the greater the soliton amplitude becomes. In addition, the value of η_{jR} influences the intensity and period of interaction. Furthermore, by choosing the different values of $p(\xi)$, solitons present the different properties and features during the interaction.

3.1.2 The effect of η_{jI}

It is notable that in Figs. 2, 5, η_{jI} is chosen to be zero. When $\eta_{jI} \neq 0$, Fig. 6 displays another situation of the pulse transmission in the DDF, where solitons undergo a fascinating change in the propagation direction. The negative and positive values chosen for η_{jI} in Figs. 6, 7, respectively, result in the changes of the velocity of solitons.

In Fig. 6, we can observe that the changes of the soliton velocity are opposite to those in Fig. 7. The soliton accelerates at first, and then decelerates in Fig. 6b. The other cases are similar with the line profile in Figs. 6, 7. Special attention should be paid to $|\eta_{jI}|$ which determines the degree of acceleration of solitons. In Fig. 7, it can be seen that the soliton velocity changes slowly owing to $\eta_{jI} = -1$. When $\eta_{jI} = -6$, Fig. 8 illustrates the effect of the soliton with the bigger acceleration as it progresses along the length of the optical fibers.

In fact, we notice that the term $\eta_2 \int p(\xi)\, d\xi$ represents the acceleration of the soliton in Solution (14). For the choice of $p(\xi)$ in Fig. 8b, the soliton velocity varies in line form with ξ. When the dispersion profile is the cosine one in Fig. 8c, the soliton velocity changes as the cosine relation. Correspondingly, Fig. 8d depicts the soliton with the dispersion profile taken as the Gaussian one.

Thus, we can conclude that the sign (positive or negative) of η_{jI} can determine the deceleration or acceleration of solitons and $|\eta_{jI}|$ determines the degree of deceleration or acceleration of them. The bigger the value of $|\eta_{jI}|$ is, the greater changes of the soliton velocity will be. Moreover, the deceleration or acceleration of solitons is consistent with the variation mode of $p(\xi)$ in the DDF, and we are able to control the velocity of solitons by managing the function forms of $p(\xi)$ in optical soliton communication systems.

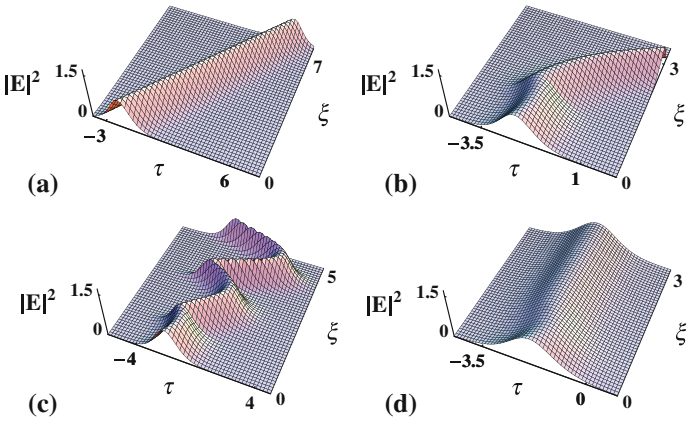

Fig. 6 Intensity profiles of the soliton via Solutions (13) with the parameters as $\Gamma(\xi) = 0.01, \eta_{1R} = \eta_{2R} = 1, \eta_{1I} = \eta_{2I} = 1, \varphi_1 = \varphi_2 = 1.8$, **a** $p(\xi) = 1$, **b** $p(\xi) = \left|1 + (\frac{1}{18} - 1)\xi\right|$, **c** $p(\xi) = \left|\cos\left[(\arccos\frac{1}{18})\,\xi\right]\right|$, **d** $p(\xi) = \left|\exp\left[-(\ln 18)\,\xi^2\right]\right|$

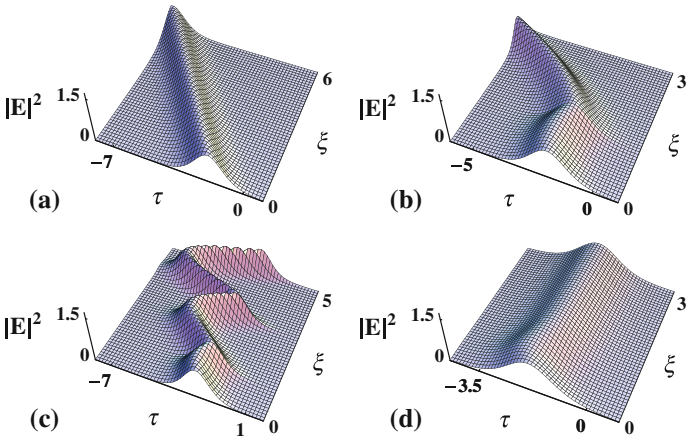

Fig. 7 Intensity profiles of the soliton via Solutions (13) with the parameters as $\Gamma(\xi) = 0.01, \eta_{1R} = \eta_{2R} = 1, \eta_{1I} = \eta_{2I} = -1, \varphi_1 = \varphi_2 = 1.8$, **a** $p(\xi) = 1$, **b** $p(\xi) = \left|1 + (\frac{1}{18} - 1)\xi\right|$, **c** $p(\xi) = \left|\cos\left[(\arccos\frac{1}{18})\,\xi\right]\right|$, **d** $p(\xi) = \left|\exp\left[-(\ln 18)\,\xi^2\right]\right|$

In the above analysis, $\eta_{1I} = \eta_{2I}$ which directly leads to the parallel incidence of the solitons. Next, the case of $\eta_{1I} \neq \eta_{2I}$ will be discussed. In Fig. 9, the most fascinating features of solitons (particle-like interaction) are displayed. To understand the interaction in a more explicit manner, we make the asymptotic analysis for Solutions (13) as follows:

(1) Before the interaction ($\xi \to -\infty$)

(a) $\theta_1 + \theta_1^* \sim 0,\ \theta_2 + \theta_2^* \to -\infty$:

$$u \to A_1 \operatorname{sech}\left(\frac{\theta_1 + \theta_1^* + \ln B_{21}}{2}\right), \tag{15}$$

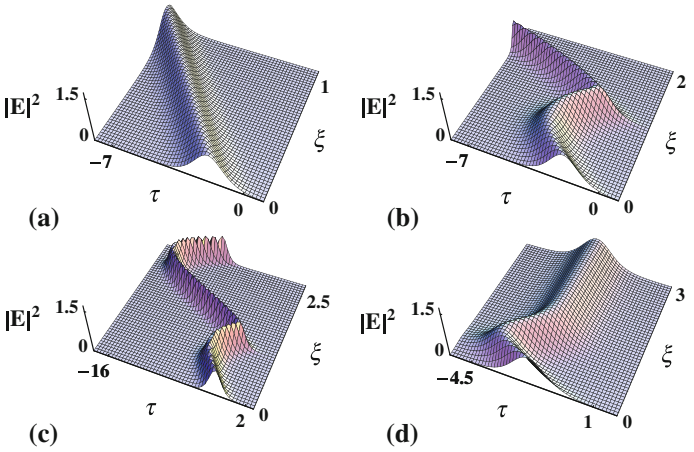

Fig. 8 Intensity profiles of the soliton via Solutions (13) with the parameters as $\Gamma(\xi) = 0.01, \eta_{1R} = \eta_{2R} = 1, \eta_{1I} = \eta_{2I} = -6, \varphi_1 = \varphi_2 = 1.8$, **a** $p(\xi) = 1$, **b** $p(\xi) = \left|1 + (\frac{1}{18} - 1)\xi\right|$, **c** $p(\xi) = \left|\cos\left[(\arccos\frac{1}{18})\,\xi\right]\right|$, **d** $p(\xi) = \left|\exp\left[-(\ln 18)\,\xi^2\right]\right|$

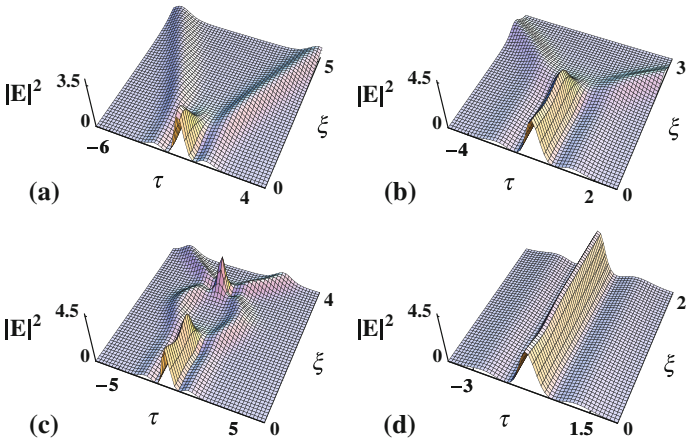

Fig. 9 Intensity profiles of solitons via Solutions (13) with the parameters as $\Gamma(\xi) = 0.01, \eta_{1R} = \eta_{2R} = 1, \eta_{1I} = 1, \eta_{2I} = -1, \varphi_1 = \varphi_2 = 1.8$, **a** $p(\xi) = 1$, **b** $p(\xi) = \left|1 + (\frac{1}{18} - 1)\,\xi\right|$, **c** $p(\xi) = \left|\cos\left[(\arccos\frac{1}{18})\,\xi\right]\right|$, **d** $p(\xi) = \left|\exp\left[-(\ln 18)\,\xi^2\right]\right|$

where $A_1 = \frac{1}{2\sqrt{B21}} \exp\left(\frac{\theta_1 - \theta_1^*}{2}\right)$. θ_1, θ_1^* and B_{21} are defined in Expressions (12)–(13).

(b) $\theta_2 + \theta_2^* \sim 0,\ \theta_1 + \theta_1^* \to \infty$:

$$u \to A_2 \mathrm{sech}\left(\frac{\theta_2 + \theta_2^* + \ln\frac{C_{21}}{B_{21}}}{2}\right), \tag{16}$$

where $A_2 = \frac{A_{21}}{2\sqrt{B_{21}C_{21}}} \exp\left(\frac{\theta_2 - \theta_2^*}{2}\right)$. $\theta_2, \theta_2^*, A_{21}, B_{21}$ and C_{21} are defined in Expressions (12)–(13).

(2) After the interaction ($\xi \to +\infty$)

(a) $\theta_1 + \theta_1^* \sim 0,\ \theta_2 + \theta_2^* \to \infty$:

$$u \to B_1 \operatorname{sech}\left(\frac{\theta_1 + \theta_1^* + \ln \frac{C_{21}}{B_{24}}}{2}\right), \tag{17}$$

where $B_1 = \frac{A_{22}}{2\sqrt{B_{24}C_{21}}} \exp\left(\frac{\theta_1 - \theta_1^*}{2}\right)$. A_{22} and B_{24} are defined in Expressions (12)–(13).

(b) $\theta_2 + \theta_2^* \sim 0,\ \theta_1 + \theta_1^* \to -\infty$:

$$u \to B_2 \operatorname{sech}\left(\frac{\theta_2 + \theta_2^* + \ln B_{24}}{2}\right), \tag{18}$$

where $B_2 = \frac{1}{2\sqrt{B_{24}}} \exp\left(\frac{\theta_2 - \theta_2^*}{2}\right)$.

According to the above expressions, it can be proven that the total energy of the solitons is conserved before and after interaction, that is,

$$|A_1|^2 + |A_2|^2 = |B_1|^2 + |B_2|^2 . \tag{19}$$

Furthermore, $|A_1|^2$, $|A_2|^2$, $|B_1|^2$ and $|B_2|^2$ are all constants for the given η_1 and η_2. Therefore, the interaction between solitons is elastic and there is only a phase shift of the soliton position. In Fig. 9, two input solitons do not keep the same phase and have an angle. The size of the angle between solitons is determined by η_{1I} and η_{2I}.

Figure 9 displays the elastic interaction of two solitons. After the interaction, they can retain their forms and structures as before even though they propagate a long distance. Because the solitons in Fig. 8c change periodically, they exhibit the periodical interaction in Fig. 9c. Specifically, two solitons generate a new soliton in Fig. 9d during their propagation. In theory, the new soliton can be eliminated without destroying the properties of input solitons if we use the phase shifter.

3.1.3 The effect of φ_j

As described above, when $\varphi_1 = \varphi_2$, two solitons interact with each other unless they have the same amplitude and incident direction. In this case, we mainly discuss the effect of φ_j shown in Fig. 10. The values of φ_1 and φ_2 in Fig. 10a are -0.5 and 1.8, respectively. If $\varphi_1 = \varphi_2$ without changing the other parameters, the propagation solitons interact with each other as seen in Fig. 2a. Now, due to the different values of φ_j, the relative distance of them will increase as the difference of the values of φ_j increase. Simultaneously, two solitons do not influence each other and propagate stably. As a special case, in Fig. 10b, solitons with the different incident directions are displayed. Soliton interaction can also be controlled by choosing the different values of φ_j when solitons propagate in the DDF with the Gaussian profile. As a consequence, we can choose the different values of φ_j to control the interaction of solitons. However, the system bandwidth may be wasted and the capacity of the systems will be decreased by increasing the relative distance of solitons.

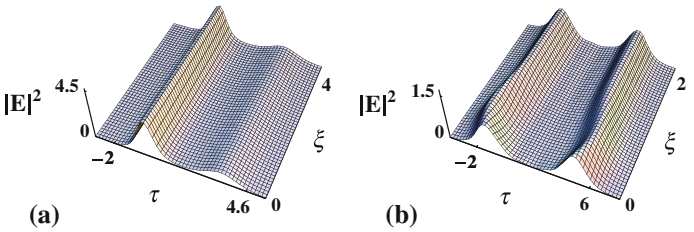

Fig. 10 Intensity profiles of solitons via Solutions (13). The parameters are $\Gamma(\xi) = 0.01$, **a** $\eta_{1R} = 1, \eta_{2R} = 2, \eta_{1I} = \eta_{2I} = 0, \varphi_1 = -0.5$ and $\varphi_2 = 1.8$, **b** $\eta_{1R} = \eta_{2R} = 1, \eta_{1I} = 2, \eta_{2I} = -2, \varphi_1 = -4, \varphi_2 = 1.8$ and $p(\xi) = \left|\exp\left[-(\ln 18)\,\xi^2\right]\right|$

3.2 Three-soliton solutions

According to the above procedure of obtaining Solutions (13), we can proceed to construct the three-soliton solutions for Eq. (1) as below:

$$u = \frac{g(\xi,\tau)}{f(\xi,\tau)} = \frac{g_1(\xi,\tau) + g_3(\xi,\tau) + g_5(\xi,\tau)}{1 + f_2(\xi,\tau) + f_4(\xi,\tau) + f_6(\xi,\tau)}, \tag{20}$$

where

$$\begin{aligned}
g_1(\xi,\tau) &= e^{\theta_1} + e^{\theta_2} + e^{\theta_3},\\
g_3(\xi,\tau) &= A_{31}e^{\theta_1+\theta_2+\theta_1^*} + A_{32}e^{\theta_1+\theta_3+\theta_1^*} + A_{33}e^{\theta_1+\theta_2+\theta_2^*} + A_{34}e^{\theta_2+\theta_3+\theta_2^*} + A_{35}e^{\theta_1+\theta_3+\theta_3^*}\\
&\quad + A_{36}e^{\theta_2+\theta_3+\theta_3^*} + A_{37}e^{\theta_2+\theta_3+\theta_1^*} + A_{38}e^{\theta_1+\theta_3+\theta_2^*} + A_{39}e^{\theta_1+\theta_2+\theta_3^*},\\
g_5(\xi,\tau) &= M_{31}e^{\theta_1+\theta_2+\theta_3+\theta_1^*+\theta_2^*} + M_{32}e^{\theta_1+\theta_2+\theta_3+\theta_2^*+\theta_3^*} + M_{33}e^{\theta_1+\theta_2+\theta_3+\theta_1^*+\theta_3^*},\\
f_2(\xi,\tau) &= B_{31}e^{\theta_1+\theta_1^*} + B_{32}e^{\theta_2+\theta_2^*} + B_{33}e^{\theta_3+\theta_3^*} + B_{34}e^{\theta_1+\theta_2^*} + B_{35}e^{\theta_2+\theta_1^*} + B_{36}e^{\theta_1+\theta_3^*}\\
&\quad + B_{37}e^{\theta_3+\theta_1^*} + B_{38}e^{\theta_2+\theta_3^*} + B_{39}e^{\theta_3+\theta_2^*},
\end{aligned}$$

$$\begin{aligned}
f_4(\xi,\tau) &= C_{31}e^{\theta_1+\theta_2+\theta_1^*+\theta_2^*} + C_{32}e^{\theta_1+\theta_3+\theta_1^*+\theta_3^*} + C_{33}e^{\theta_2+\theta_3+\theta_2^*+\theta_3^*} + C_{34}e^{\theta_1+\theta_2+\theta_1^*+\theta_3^*}\\
&\quad + C_{35}e^{\theta_1+\theta_3+\theta_1^*+\theta_2^*} + C_{36}e^{\theta_1+\theta_2+\theta_2^*+\theta_3^*} + C_{37}e^{\theta_2+\theta_3+\theta_1^*+\theta_2^*} + C_{38}e^{\theta_1+\theta_3+\theta_2^*+\theta_3^*}\\
&\quad + C_{39}e^{\theta_2+\theta_3+\theta_1^*+\theta_3^*},\\
f_6(\xi,\tau) &= Q_3 e^{\theta_1+\theta_2+\theta_3+\theta_1^*+\theta_2^*+\theta_3^*},
\end{aligned}$$

$$\begin{aligned}
A_{31} &= \frac{(\eta_1-\eta_2)^2}{(\eta_1+\eta_1^*)^2(\eta_2+\eta_1^*)^2},\ A_{32} = \frac{(\eta_1-\eta_3)^2}{(\eta_1+\eta_1^*)^2(\eta_3+\eta_1^*)^2},\ A_{33} = \frac{(\eta_1-\eta_2)^2}{(\eta_1+\eta_2^*)^2(\eta_2+\eta_2^*)^2},\\
A_{34} &= \frac{(\eta_2-\eta_3)^2}{(\eta_2+\eta_2^*)^2(\eta_3+\eta_2^*)^2},\ A_{35} = \frac{(\eta_1-\eta_3)^2}{(\eta_1+\eta_3^*)^2(\eta_3+\eta_3^*)^2},\ A_{36} = \frac{(\eta_2-\eta_3)^2}{(\eta_2+\eta_3^*)^2(\eta_3+\eta_3^*)^2},\\
A_{37} &= \frac{(\eta_2-\eta_3)^2}{(\eta_2+\eta_1^*)^2(\eta_3+\eta_1^*)^2},\ A_{38} = \frac{(\eta_1-\eta_3)^2}{(\eta_1+\eta_2^*)^2(\eta_3+\eta_2^*)^2},\ A_{39} = \frac{(\eta_1-\eta_2)^2}{(\eta_1+\eta_3^*)^2(\eta_2+\eta_3^*)^2},
\end{aligned}$$

$$\begin{aligned}
B_{31} &= \frac{1}{(\eta_1+\eta_1^*)^2},\ B_{32} = \frac{1}{(\eta_2+\eta_2^*)^2},\ B_{33} = \frac{1}{(\eta_3+\eta_3^*)^2},\\
B_{34} &= \frac{1}{(\eta_1+\eta_2^*)^2},\ B_{35} = \frac{1}{(\eta_2+\eta_1^*)^2},\ B_{36} = \frac{1}{(\eta_1+\eta_3^*)^2},\\
B_{37} &= \frac{1}{(\eta_3+\eta_1^*)^2},\ B_{38} = \frac{1}{(\eta_2+\eta_3^*)^2},\ B_{39} = \frac{1}{(\eta_3+\eta_2^*)^2},
\end{aligned}$$

$$C_{31}=\frac{(\eta_1-\eta_2)^2(\eta_1^*-\eta_2^*)^2}{(\eta_1+\eta_1^*)^2(\eta_1+\eta_2^*)^2(\eta_2+\eta_1^*)^2(\eta_2+\eta_2^*)^2},$$

$$C_{32}=\frac{(\eta_1-\eta_3)^2(\eta_1^*-\eta_3^*)^2}{(\eta_1+\eta_1^*)^2(\eta_1+\eta_3^*)^2(\eta_3+\eta_1^*)^2(\eta_3+\eta_3^*)^2},$$

$$C_{33}=\frac{(\eta_2-\eta_3)^2(\eta_2^*-\eta_3^*)^2}{(\eta_2+\eta_2^*)^2(\eta_2+\eta_3^*)^2(\eta_3+\eta_2^*)^2(\eta_3+\eta_3^*)^2},$$

$$C_{34}=\frac{(\eta_1-\eta_2)^2(\eta_1^*-\eta_3^*)^2}{(\eta_1+\eta_1^*)^2(\eta_1+\eta_3^*)^2(\eta_2+\eta_1^*)^2(\eta_2+\eta_3^*)^2},$$

$$C_{35}=\frac{(\eta_1-\eta_3)^2(\eta_1^*-\eta_2^*)^2}{(\eta_1+\eta_1^*)^2(\eta_1+\eta_2^*)^2(\eta_3+\eta_1^*)^2(\eta_3+\eta_2^*)^2},$$

$$C_{36}=\frac{(\eta_1-\eta_2)^2(\eta_2^*-\eta_3^*)^2}{(\eta_1+\eta_2^*)^2(\eta_1+\eta_3^*)^2(\eta_2+\eta_2^*)^2(\eta_2+\eta_3^*)^2},$$

$$C_{37}=\frac{(\eta_2-\eta_3)^2(\eta_1^*-\eta_2^*)^2}{(\eta_2+\eta_1^*)^2(\eta_2+\eta_2^*)^2(\eta_3+\eta_1^*)^2(\eta_3+\eta_2^*)^2},$$

$$C_{38}=\frac{(\eta_1-\eta_3)^2(\eta_2^*-\eta_3^*)^2}{(\eta_1+\eta_2^*)^2(\eta_1+\eta_3^*)^2(\eta_3+\eta_2^*)^2(\eta_3+\eta_3^*)^2},$$

$$C_{39}=\frac{(\eta_2-\eta_3)^2(\eta_1^*-\eta_3^*)^2}{(\eta_2+\eta_1^*)^2(\eta_2+\eta_3^*)^2(\eta_3+\eta_1^*)^2(\eta_3+\eta_3^*)^2},$$

$$M_{31}=\frac{(\eta_1-\eta_2)^2(\eta_1-\eta_3)^2(\eta_2-\eta_3)^2(\eta_1^*-\eta_2^*)^2}{(\eta_1+\eta_1^*)^2(\eta_1+\eta_2^*)^2(\eta_2+\eta_1^*)^2(\eta_2+\eta_2^*)^2(\eta_3+\eta_1^*)^2(\eta_3+\eta_2^*)^2},$$

$$M_{32}=\frac{(\eta_1-\eta_2)^2(\eta_1-\eta_3)^2(\eta_2-\eta_3)^2(\eta_2^*-\eta_3^*)^2}{(\eta_1+\eta_2^*)^2(\eta_1+\eta_3^*)^2(\eta_2+\eta_2^*)^2(\eta_2+\eta_3^*)^2(\eta_3+\eta_2^*)^2(\eta_3+\eta_3^*)^2},$$

$$M_{33}=\frac{(\eta_1-\eta_2)^2(\eta_1-\eta_3)^2(\eta_2-\eta_3)^2(\eta_1^*-\eta_3^*)^2}{(\eta_1+\eta_1^*)^2(\eta_1+\eta_3^*)^2(\eta_2+\eta_1^*)^2(\eta_2+\eta_3^*)^2(\eta_3+\eta_1^*)^2(\eta_3+\eta_3^*)^2},$$

$$Q_3=\frac{(\eta_1-\eta_2)^2(\eta_1-\eta_3)^2(\eta_2-\eta_3)^2}{(\eta_1+\eta_1^*)^2(\eta_1+\eta_2^*)^2(\eta_1+\eta_3^*)^2(\eta_2+\eta_1^*)^2(\eta_2+\eta_2^*)^2}\times\frac{(\eta_1^*-\eta_2^*)^2(\eta_1^*-\eta_3^*)^2(\eta_2^*-\eta_3^*)^2}{(\eta_2+\eta_3^*)^2(\eta_3+\eta_1^*)^2(\eta_3+\eta_2^*)^2(\eta_3+\eta_3^*)^2},$$

with $\theta_j=\eta_j\,\tau+k_j(\xi)+\varphi_j$, $\eta_j=\eta_{jR}+i\,\eta_{jI}$ and $k_j(\xi)=k_{jR}(\xi)+i\,k_{jI}(\xi)$ $(j=1,2,3)$ with η_{jR}, η_{jI}, φ_j as real constants and

$$k_{jR}(\xi)=-\eta_{jR}\,\eta_{jI}\int p(\xi)\,d\xi,\quad k_{jI}(\xi)=\frac{\left(\eta_{jR}^2-\eta_{jI}^2\right)}{2}\int p(\xi)\,d\xi.$$

In Solutions (20), if $\eta_{1R}=\eta_{2R}=\eta_{3R}$, $\eta_{1I}=\eta_{2I}=\eta_{3I}=0$ and $\varphi_1=\varphi_2=\varphi_3$, the three-soliton solution changes into Solutions (14). However, if the parameters do not meet the above conditions, the three solitons display a complex relation during the propagation. Figure 11a displays the unaffected propagation among three solitons due to the large difference values of φ_j. Three parallel solitons transmit stably and propagate along the optical fibers with a constant separation among them. On the contrary, when reducing the difference value of φ_j, the three solitons interact with each other periodically in Figs. 11b, c, d.

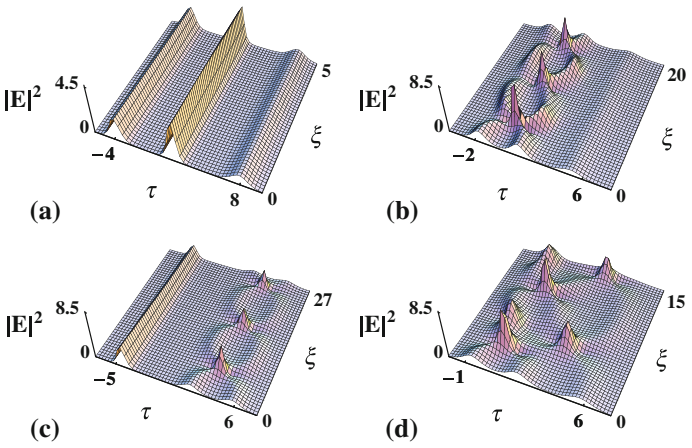

Fig. 11 Intensity profiles of solitons via Solutions (20). The parameters are $\Gamma(\xi) = 0.01$, $\eta_{1R} = 1$, $\eta_{2R} = 2$, $\eta_{3R} = 1.5$, $\eta_{1I} = \eta_{2I} = \eta_{3I} = 0$, $p(\xi) = 1$, **a** $\varphi_1 = -1.8$, $\varphi_2 = 1.8$ and $\varphi_3 = 6.8$, **b** $\varphi_1 = 1$ and $\varphi_2 = \varphi_3 = 3$, **c** $\varphi_1 = 0.5$, $\varphi_2 = 10$ and $\varphi_3 = 0.8$, **d** $\varphi_1 = 0.6$, $\varphi_2 = 1$ and $\varphi_3 = 0.8$

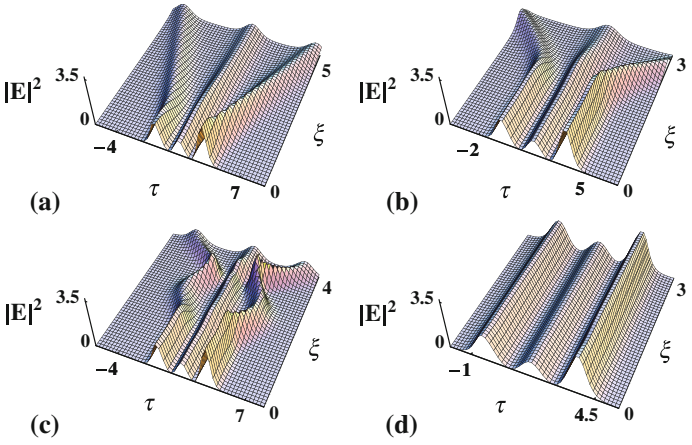

Fig. 12 Intensity profiles of solitons via Solutions (20). The parameters are $\Gamma(\xi) = 0.01$, $\eta_{1R} = \eta_{2R} = \eta_{3R} = 1$, $\eta_{1I} = 1$, $\eta_{2I} = 0$, $\eta_{3I} = -1$, $\varphi_1 = \varphi_2 = \varphi_3 = 0$, **a** $p(\xi) = 1$, **b** $p(\xi) = \left|1 + (\frac{1}{18} - 1)\xi\right|$, **c** $p(\xi) = \left|\cos\left[(\arccos\frac{1}{18})\,\xi\right]\right|$, **d** $p(\xi) = \left|\exp\left[-(\ln 18)\,\xi^2\right]\right|$

Similar to Fig. 9, when the incident solitons are inputed with different phases, they present some new features. In Fig. 12a, b, they collide elastically with different shifts among the soliton centers. After the interaction, they are well separated and remain original shapes and velocities of their own. Of course, those three solitons also comply with the energy conservation law in the process of propagation in this system.

Figure 12c shows another interaction scenario. Because $p(\xi)$ is the cosine function, the periodical variations of soliton interaction occur when $\eta_{jI} \neq 0$. Interestingly, solitons propagate without interacting in the DDF with the Gaussian profile even though there are no intervals among them in Fig. 12d. That might be of potential application in communication systems which can enhance the capacity of systems.

4 Conclusions

In conclusion, we have investigated Eq. (1), which can be used to describe the solitons propagation in an inhomogeneous optical fiber. With the aid of symbolic computation, we have carried out our study from an analytic view. With the Hirota method and symbolic computation, the analytic Two- and Three-Soliton Solutions (13) and (20) for Eq. (1) have been obtained. Of physical and optical interests, relevant properties and features of solitons in the DDF with different kinds of dispersion profiles have been analyzed and graphically discussed. The velocities of solitons under certain conditions can be controlled using the DDF with different profiles, as seen in Figs. 6–8. In addition, through making an asymptotic analysis via Expressions (15)–(18) for Solutions (13), we have found that the interaction between two solitons is elastic and the total energy is conserved in the system. Finally, a new approach to control the soliton interaction using the DDF with the Gaussian profile has been suggested through different values of the parameters, as seen in Fig. 12(d) . Attention should be drawn as below:

(1) Compared with the earlier reports, it is worth noting that, to our knowledge, the function $p(\xi)$ chosen as the dispersion profile of the DDF is first reported. The DDF with the Gaussian profile can be used in the non-interacting solitons systems, for the solitons propagate stably and do not influence each other even though there are no intervals among them, as seen in Fig. 12(d).

(2) The soliton undergoes the change in its velocity, as seen in Figs. 6–8 which has potential applications in the design of high-speed optical devices and ultralarge capacity transmission systems. That means that we are able to control the velocity and amplitude of solitons using the DDF with the selected values of the parameters. We expect that the above phenomena could be observed in the experiments.

The results could be hopefully of certain value in controlling the information sequences of ultrashort pulses in fiber communication lines through the control of their interaction.

Acknowledgments This work has been supported by the National Natural Science Foundation of China under Grant No. 60772023, by the Fundamental Research Funds for the Central Universities of China (Grant Nos. 2011RCZJ06 and 2011BUPTYB02), by the Specialized Research Fund for the Doctoral Program of Higher Education (No. 200800130006), Chinese Ministry of Education, and by the National Basic Research Program of China (Grant No. 2010CB923200).

References

Agrawal, G.P.: Nonlinear Fiber Optics, 4th edn. Academic Press, San Diego (2007)

Chen, S.H., Liu, H.P., Zhang, S.W., Yi, L.: Compression of Hermite–Gaussian pulses in an engineered optical fiber absorber with varying dispersion and nonlinearity. Phys. Lett. A **353**, 493–496 (2006)

Gao, Y.T., Tian, B.: Variable-coefficient higher-order nonlinear Schrödinger model in optical fibers: variable-coefficient bilinear form, Bäcklund transformation, brightons and symbolic computation. Phys. Lett. A **366**, 223–229 (2007)

Ganapathy, R., Porsezian, K., Hasegawa, A., Serkin, V.N.: Soliton interaction under soliton dispersion management. IEEE J. Quantum Electron. **44**, 383–390 (2008)

Georges, T., Favre, F.: Modulation, filtering, and initial phase control of interacting solitons. J. Opt. Soc. Am. B **10**, 1880–1889 (1993)

Han, S.H., Park, Q.H.: Effect of self-steepening on optical solitons in a continuous wave background. Phys. Rev. E **83**, 066601-1–6 (2011)

Hasegawa, A., Tappert, F.: Transmission of stationary nonlinear optical pulses in dispersive dielectric fiber, I. Anomalous dispersion. Appl. Phys. Lett. **23**, 142–144 (1973a)

Hasegawa, A., Tappert, F.: Transmission of stationary nonlinear optical pulses in dispersive dielectric fiber, II. Normal dispersion. Appl. Phys. Lett. **23**, 171–172 (1973b)
Hasegawa, A., Matsumoto, M.: Optical Solitons in Fibers. 3rd edn. Springer, Berlin (2003)
Hirota, R.: Exact solution of the KdV equation for multiple collisions of solitons. Phys. Rev. Lett. **27**, 1192–1194 (1971)
Hirota, R.: Exact envelope-soliton of a nonlinear wave equation. J. Math. Phys. **14**, 805–814 (1973)
Inoue, T., Sugahara, H., Maruta, A., Kodama, Y.: Interactions between dispersion managed solitons in optical-time-division-multiplexed system. IEEE Photon. Technol. Lett. **12**, 299–301 (2000)
Joshi, N.: Painlevé property of general variable-coefficient versions of the Kortewegde Vries and nonlinear Schrödinger equations. Phys. Lett. A **125**, 456–460 (1987)
Kanna, T., Tsoy, E.N., Akhmediev, N.: On the solution of multicomponent nonlinear Schrödinger equations. Phys. Lett. A **330**, 224–229 (2004)
Kivshar, Y.S., Agrawal, G.P.: Optical Solitons: From Fibers to Photonic Crystals. Academic Press, San Diego (2003)
Kodama, Y., Nozaki, L.: Soliton interaction in optical fibres. Opt. Lett. **12**, 1038–1040 (1987)
Komarova, A., Komarov, K., Leblond, H., Sanchez, F.: Spectral management of solitons interaction and generation regimes of fiber laser. ICTON **1**, 217–220 (2007)
Kubota, H., Nakazawa, M.: Soliton transmission control in time and frequency domains. IEEE J. Quantum Electron. **29**, 2189–2197 (1993)
Kurokawa, K., Kubota, H., Nakazawa, M.: Femtosecond soliton interactions in a distributed erbium-doped fiber amplifier. IEEE J. Quantum Electron. **30**, 2220–2226 (1994)
Lakoba, T.I., Agrawal, G.P.: Optimization of the average-dispersion range for longhaul dispersion-managed soliton systems. IEEE J. Lightw. Technol. **18**, 1504–1512 (2000)
Li, B., Chen, Y.: On exact solutions of the nonlinear Schrödinger equations in optical fiber. Chaos Solitons Fractals **21**, 241–247 (2004)
Luo, H.G., Zhao, D., He, X.G.: Exactly controllable transmission of nonautonomous optical solitons. Phys. Rev. A **79**, 063802-1–4 (2009)
Mollenauer, L.F., Stolen, R.H., Gordon, J.P.: Experimental observation of picosecond pulse narrowing and solitons in optical fibers. Phys. Rev. Lett. **45**, 1095–1098 (1980)
Morita, I., Tanaka, K., Edagawa, N., Suzuki, M.: 40 Gb/s single-channel soliton transmission over transoceanic distances by reducing Gordon–Haus timing jitter and soliton–soliton interaction. IEEE J. Lightw. Technol. **17**, 2506–2511 (1999)
Pinto, A.N., Agrawal, G.P., da Rocha, J.F.: Effect of soliton interaction on timing jitter in communication systems. IEEE J. Lightw. Technol. **16**, 515–519 (1998)
Ponomarenko, S.A., Agrawal, G.P.: Optical similaritons in nonlinear waveguides. Opt. Lett. **32**, 1659–1661 (2007)
Porsezian, K., Ganapathy, R., Hasegawa, A., Serkin, V.N.: Nonautonomous soliton dispersion management. IEEE J. Quantum Electron. **45**, 1577–1583 (2009)
Pusch, A., Hamm, J.M., Hess, O.: Femtosecond nanometer-sized optical solitons. Phys. Rev. A **84**, 023827-1–5 (2011)
Serkin, V.N., Hasegawa, A.: Novel soliton solutions of the nonlinear Schrödinger equation model. Phys. Rev. Lett. **85**, 4502–4505 (2000)
Serkin, V.N., Hasegawa, A.: Exactly integrable nonlinear Schrödinger equation models with varying dispersion, nonlinearity and gain: application for soliton dispersion. IEEE J. Sel. Top. Quantum Electron. **8**, 418–431 (2002)
Serkin, V.N., Hasegawa, A., Belyaeva, T.L.: Nonautonomous solitons in external potentials. Phys. Rev. Lett. **98**, 074102-1–4 (2007)
Sun Z.Y., Gao, Y.T., Yu, X., Liu, W.J., Liu, Y.: Bound vector solitons and soliton complexes for the coupled nonlinear Schrödinger equations. Phys. Rev. E **80**, 066608 (2009)
Sun, Z.Y., Gao, Y.T., Yu, X., Liu, Y.: Formation of vortices in a combined pressure-driven electro-osmotic flow through the insulated sharp tips under finite Debye length effects. Colloid Surf. A **366**, 1 (2010)
Tian, B., Gao, Y.T.: Symbolic-computation study of the perturbed nonlinear Schrödinger model in inhomogeneous optical fibers. Phys. Lett. A **342**, 228–236 (2005)
Turitsyn, S.K., Smyth, N.F., Turitsyna, E.G.: Solitary waves in nonlinear dispersive systems with zero average dispersion. Phys. Rev. E **58**, R44–R47 (1998)
Wabnitz, S., Kodama, Y., Aceves, A.B.: Control of optical soliton interactions. Opt. Fiber Technol. **1**, 187–217 (1995)
Wai, P.K., Cao, W.H.: Ultrashort soliton generation through higher-order soliton compression in a nonlinear optical loop mirror constructed from dispersion-decreasing fiber. J. Opt. Soc. Am. B **20**, 1346–1355 (2003)

Wang, L., Gao, Y.T., Gai, X.L., Sun, Z.Y.: Inelastic interactions and double Wronskian solutions for the Whitham-Broer-Kaup model in shallow water. Phys. Scr. **80**, 065017 (2009)
Wang, L., Gao, Y.T., Qi, F.H.: Multi-solitonic solutions for the variable-coefficient variant Boussinesq model of the nonlinear water waves. J. Math. Anal. Appl. **372**, 110 (2010)
Wang, L.Y., Li, L., Li, Z.H., Zhou, G.S., Mihalache, D.: Generation, compression and propagation of pulse trains in the nonlinear Schrödinger equation with distributed coefficients. Phys. Rev. E **72**, 036614-1–7 (2005)
Wu, L., Zhang, J.F., Li, L., Finot, C., Porsezian, K.: Similariton interactions in nonlinear graded-index waveguide amplifiers. Phys. Rev. A **78**, 053807-1–7 (2008)
Xie, C.J., Karlsson, M., Andrekson, P.A., Sunnerud, H., Li, J.: Influences of polarization-mode dispersion on soliton transmission systems. J. Sel. Top. Quantum Electron. **8**, 575–590 (2002)
Yu, X., Gao, Y.T., Sun, Z.Y., Liu, Y.: N-soliton solutions, Backlund transformation and Lax pair for a generalized variable-coefficient fifth-order Korteweg-de Vries equation. Physica Scripta **81**, 045402 (2010)
Yu, X., Gao, Y.T., Sun, Z.Y., Liu, Y.: Solitonic propagation and interaction for a generalized variable coefficient forced Korteweg-de Vries equation in fluids. Phys. Rev. E **83**, 056601 (2011)
Zhang, J.F., Dai, C.Q., Yang, Q., Zhu, J.M.: Variable-coefficient F-expansion method and its application to nonlinear Schrödinger equation. Opt. Commun. **252**, 408–421 (2005)